

Rosetta-Philae RF link, from separation to hibernation

Clément Dudal, Céline Loisel, Emmanuel Robert
CNES

18 avenue Edouard Belin 31401 Toulouse Cedex 9 France; +33561283070
clement.dudal@cnes.fr, celine.loisel@cnes.fr, emmanuel.robert@cnes.fr

Miguel Fernandez, Yves Richard, Gwenaël Guillois
Syrlinks

rue des Courtillons, ZAC de Cicé-Blossac, 35170 Bruz, France;
miguel.fernandez@syrlinks.com, yves.richard@syrlinks.com, gwenael.guillois@syrlinks.com

ABSTRACT

The Rosetta spacecraft reached the vicinity of the comet 67P/Churyumov-Gerasimenko in 2014 and released the lander Philae for an in-situ analysis through ten scientific instruments. The analysis of the lander RF link telemetry reveals major information on the lander behavior and environment during the 50-hour mission on the comet.

INTRODUCTION

The ESA/CNES/DLR Rosetta spacecraft was launched in March 2004 with the objective to reach the comet 67P/Churyumov-Gerasimenko 10 years later. One of its main assignments was to carry out in-situ analysis using Philae, a small lander of about 100 kg equipped with scientific instruments. The S-Band RF link between Rosetta and Philae was, after separation, the only mean of communication with the lander. This paper proposes an analysis of the RF link telemetry during the Separation, Descent and Landing phase (SDL) and during the First Science Sequence after landing (FSS). As the comet landing was epic, the descent and landing are studied in two different parts. A cross-comparison of our analysis is made with the one of other scientific teams to strengthen the raised conclusions.

ROSETTA-PHILAE RF LINK OVERVIEW

The transceiver is a full duplex S-band transmission set for digital data developed specifically for space applications. The conception made by Syrlinks was done with drastic objectives for mass and power consumption. For this, the use of commercial parts was decided leading to a low cost product widely used afterwards on the Myriade platform family. The transceiver is composed of a transmitter, a receiver and a reception filter for dual antenna use (Figure 1). The filter protects the receiver from out-of-band signals, particularly from the transmitter. The two functions (receiver and transmitter) are fully independent and can be activated separately. Technical details are given in the Table 1 and an illustration in Figure 2.

Table 1: Transceiver technical details

Mass	950 g
Volume	160 mm x 120 mm x 40 mm
Power consumption (28 V power bus)	1.7 W Rx only 6.5 W Rx/Tx at 20°C (1 W RF output power)
Temperature	Operational: -40°C to +50°C
Radiation	10 krad (cumulated doses)
Frequency	Telecommand link: 2208 MHz Telemetry link: 2033.2 MHz
Modulation	QPSK
Data filtering	Differential coding Nyquist half raised cosine filtering (roll-off is 0.35 in Rx, 1 in Tx)
Data rate	Telecommand link 16000 bps Telemetry link 16384 bps
Rx sensitivity range	-50/-120 dBm
Channel coding	Tx: convolutional coding (L=7, R=1/2) Rx: Viterbi soft decision decoding
Electrical interfaces	RS 485 and CMOS

There are two transceivers on both sides of the RF link. The redundancy is activated with RF switches on orbiter side (1 Tx/1 Rx active) and with diplexer on lander side (1 Tx/2 Rx active).

The choice of implementing identical RF chains for transmission and reception on the orbiter and the lander has given great advantages, such as cutting procurement costs and simplifying qualification, integration and testing.

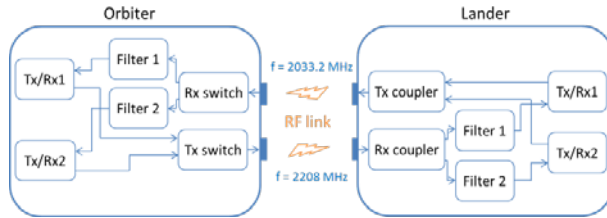


Figure 1: Rosetta-Philae bidirectionnal RF link

With 1W RF output power and 1 dBi gain (@ 60°) patch antennas, link establishment is possible for distances up to 150 km.

The lander telecommunication system answers to a request-to-send protocol from the orbiter at any time. This handshake protocol, which implies full duplex equipment and which was specifically designed for Rosetta mission ensures a desired quality of transmission even when the relative geometry and visibility between the orbiter and the lander is not favourable.



Figure 2: Rosetta ISL transceiver

In the housekeeping telemetry available at orbiter side, one parameter is particularly interesting to get information beyond its intrinsic value: the Received Signal Strength Indicator (RSSI). From this raw telemetry value, it is possible to extract the received power level on orbiter side, which can be then processed as shown in the following parts.

SEPARATION AND DESCENT

Before separation, several milestones had to be respected in order to deliver the lander in optimal conditions. Despite some late complications on the battery heating, the separation of the lander occurred nominally at 8h35 UTC. Before being able to establish the RF link, the Rosetta spacecraft had to maneuver to point its Inter Satellite Link (ISL) antennas toward the lander, leading to an AOS roughly 2 hours after separation.

The link was established within 5 min, as expected, and lasted during the 5 remaining hours of descent. It has allowed the transmission of the CIVA (Comet Infrared

and Visible Analyzer) and ROLIS (Rosetta Lander Imaging System) photographs taken before touchdown.

As expected with increasing distance between the lander and the orbiter, the RSSI decreases over time (Figure 3).



Figure 3: RSSI level during the descent toward the comet

Independently of the global decreasing level, low frequency oscillations are noticeable on the RSSI, of an average duration of 59 min (orange lines on the Figure 3). It could be explained with a multipath effect on the orbiter structure.

LANDING

The touchdown on the chosen landing site Agilkia was expected at 15h34m10 UTC and occurred with a precision of a few seconds. After touchdown, despite the announced activation success of the anchoring system, the received RF link telemetry indicated multiple and regular interruptions during two hours. The investigation carried out helped to establish the failure of the anchoring system, causing Philae to rebound on the comet surface. There were two rebounds before stabilization on the ground; they are studied from a RF point of view below.

First rebound

After first touchdown (TD1), the lander rebounded and moved away from the landing site. According to other instrument teams, it tumbled around the 3 axis keeping a relatively stable position around Z-axis. The rebound lasted roughly 2 hours. During this period, the RF link suffered multiple and periodic interruptions. The estimated RSSI on telemetry link presents high and fast variations in the range -80 dBm/-120 dBm reaching the limit of the Rx sensitivity range and leading to those link interruptions.

After first touchdown (TD1), the lander rebounded and moved away from the landing site. According to other instrument teams, it tumbled around the 3 axis keeping a relatively stable position around Z-axis. The rebound lasted roughly 2 hours. During this period, the RF link suffered multiple and periodic interruptions. The estimated RSSI on telemetry link presents high and fast

variations in the range -80 dBm/-120 dBm reaching the limit of the Rx sensitivity range and leading to those link interruptions.

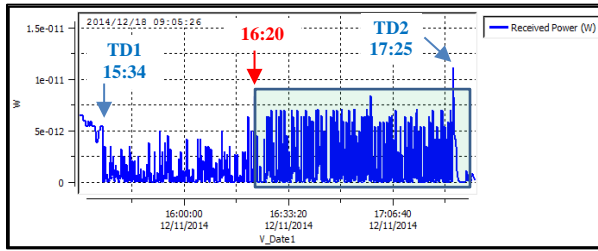


Figure 4: RSSI level during first rebound

At 16h20 UTC being 45 min after touchdown, a change is observed on the RSSI profile (**Figure 4**). The maximum measured value is roughly twice higher. The lander motion is directly responsible for this change and particularly the spin around the Z axis created during the separation. An analysis in the frequency domain provides more information on any periodical phenomenon like a spin motion and its value.

The orbiter telemetry is sampled at $F_s = 0.1$ Hz (1 sample every 10 s). According to Shannon theorem, the maximum frequency for a possible well-sampled phenomenon is 0.05 Hz (Period of 20 s). For faster phenomena, aliasing occurs and the frequency of the phenomenon must be interpreted according to the sampling frequency F_s . For a periodic phenomenon at a frequency F higher than $F_s/2$, the observed frequency will be $F_o = F_s - F$.

The Fourier Transform of the RSSI (averaged periodogram with $N_{fft} = 128$) is computed and analyzed over the period of the first rebound (**Figure 5**).

- Before 16h20, a periodic phenomenon is identified at a frequency of 0.0194 Hz (period = 51.5 s). If this measure corresponds actually to a faster phenomenon and is biased with aliasing, taking into account the sampling frequency, the real frequency would be 0.0806 Hz (period = 12.41 s).
- After 16h20, a periodic phenomenon at a frequency of 0.044 Hz (period = 22.7 s) is identified. If this measure corresponds actually to a faster phenomenon and is biased with aliasing, taking into account the sampling frequency, the real frequency would be 0.056 Hz (period = 17.86 s).

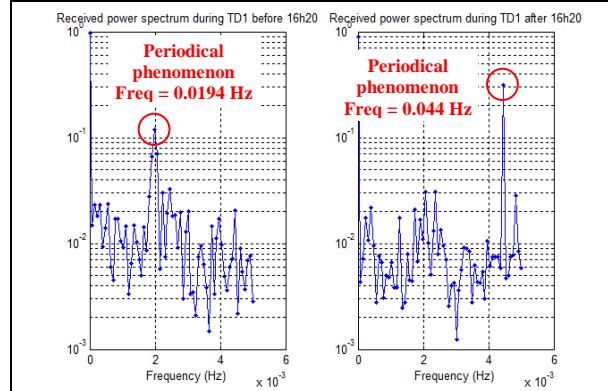


Figure 5: RSSI spectrum during first rebound, before and after 16h20

In order to solve the ambiguity on the aliasing effect, a cross-comparison is made with ROMAP (Rosetta Magnetometer and Plasma-monitor) team analysis. According to them, at 16h20, the lander may have collided with a surface feature which had for effect to slow the lander spin around its Z-axis, changing from 13 s per rotation to 24 s per rotation. It probably also reduced the lander tumbling, decreasing the dispersion around the spin axis. The lander antennas were then better pointed leading to a better signal reception on orbiter side.

Table 2: Comparison of ROMAP and RF analysis

Timeline	ROMAP	RF analysis
Before 16h20	Lander spin at 13 s/rot	Phenomenon of period 12.41 s detected
After 16:20	Lander spin at 24 s/rot	Phenomenon of period of 22.7 s detected

This allows concluding that the periodical phenomenon observed before 16h20 is actually biased with aliasing and represents the lander spin at 13 s per rotation. The spin decrease at 16h20 is perfectly visible in the analysis.

This template has been set up with several features to make it easier for you to format your paper properly. These features are described in the subsections that follow.

Second rebound

The second touchdown (TD2) occurred at 17:25:25 UTC and the lander did not stabilized on the ground leading to a second rebound of 5 min 50 s during which the RF link still suffered from interruptions but with two significant stable periods (see **Figure 6**). The presence of stable RF link periods gives indication of a favorable trend toward lander stabilization. The

instability may be due to masking of the lander antennas or multipath interference as the lander was still in motion.

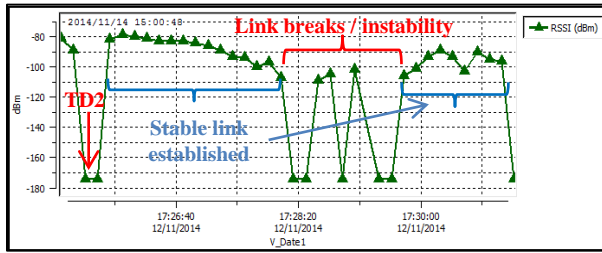


Figure 6: RSSI level during second rebound

After second rebound

The final stabilization on the comet ground occurred at 17:31:17 UTC being only 30 min before the end of the RF visibility. Typical instability is thus observed before the complete loss of the link (Figure 7). The RSSI frequency analysis does not bring much information as the lander is now stable on the ground. Nevertheless, the maximum measured level shows that a high attenuation affects the link compared to previous transmissions. This might be due to the actual lander attitude on the ground and its surrounding environment. The proximity of the lander stabilization time with the end of the visibility window does not allow concluding properly on the lander situation.

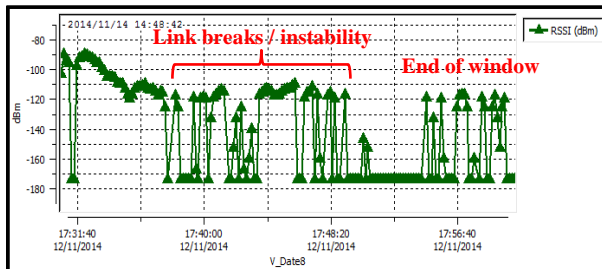


Figure 7: RSSI after stabilization on the ground

However, the analysis of the Lander antennas temperature gives precious information on the lander illumination during the rebound phase (Figure 8). The changes in illumination, particularly after stabilization on the ground, indicate that the lander is in a dark place with very low solar flux leading to a fast decrease of the antennas temperature.

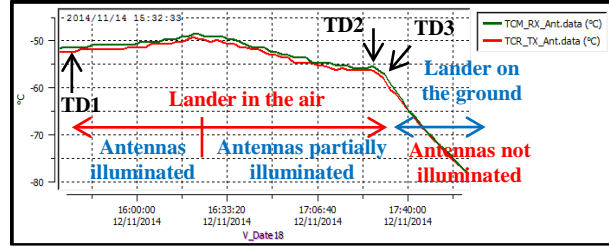


Figure 8: Lander antennas temperature from first touchdown up to end of RF visibility window

At the end of the RF visibility window, after the stabilization on the ground, two crucial questions remained unanswered: what are the final location and attitude of the lander? When the RF link will be established again to start the First Science Sequence?

FIRST SCIENCE SEQUENCE

After separation, descent and landing, the science operations were planned in two phases depending on the power supply source:

- The First Science Sequence (FSS) began at lander touchdown and ended when primary and secondary batteries were empty. The foreseen lifetime was about 50 hours.
- The Long Term Science (LTS) will begin at the 1st battery recharging and last till the end of the lander mission (thermic and power supply problematic)

Due to the unexpected landing circumstances, there was an uncertainty on the RF link re-establishment. Fortunately, the orbiter detected a signal from the lander at the predicted time for the nominal landing site. Despite the observed instability at the beginning, the FSS could start.

During the FSS, there were four RF visibilities. The overall duration of each visibility (including unstable and stable periods) decreased over time but the stability duration increased over time.

Table 3: RF visibilities characteristics during FSS

Parameter	Visi 1	Visi 2	Visi 3	Visi 4
Date (jj/mm)	13/11	13/11	14/11	14/11
Whole link duration (hh:mm)	03:57	03:42	02:48	02:22
Stable link duration (hh:mm)	02:43	02:36	02:46	02:09
Stability ratio (%)	69%	71%	99%	91%
Maximum received power on orbiter side (dBm)	-89	-91	-94	-94

The maximum measured power depends on the orbiter and lander attitudes and on the distance between them. The distance has increased continuously during the FSS which led to a higher free space path loss and a lower received power. The levels are nonetheless in a nominal range considering the simulated link budget and demonstrate a nominal transmission.

The RSSI profiles during the four visibilities are given on **Figure 9**. They show the distribution between instability and stability periods. During the stable period, arches are noticeable. They reflect the multipath interferences due to the surrounding relief.

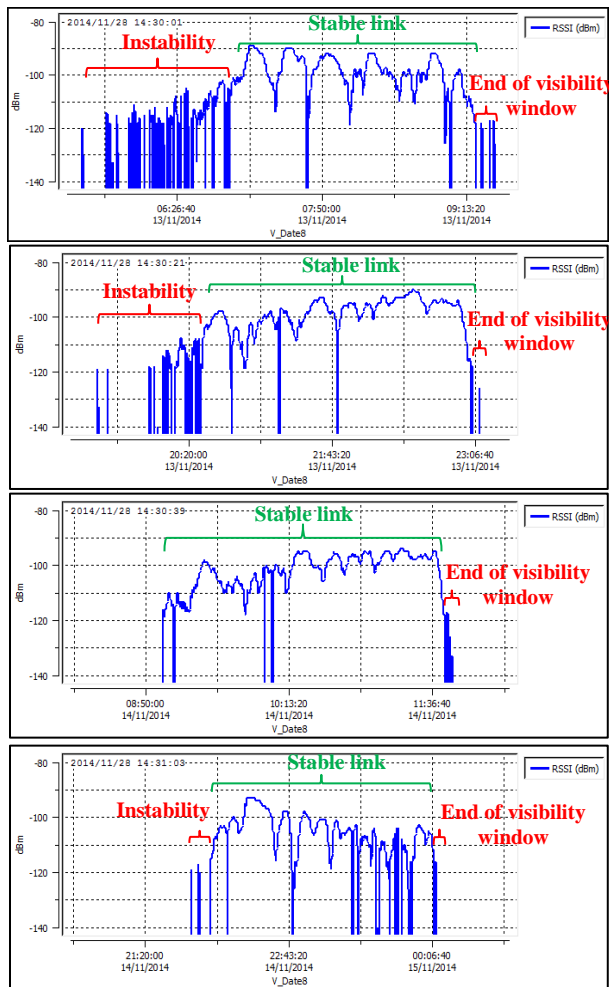


Figure 9: RSSI profiles during the four RF visibilities - first to last

The first and fourth visibilities present the same profile with a decreasing peak power level during the stable link duration. Inversely, the second and third present an increasing peak power profile.

The orbiter trajectories with regard to the lander position on the comet were then probably similar for first and fourth, and for second and third.

This conclusion is corroborated by the simulations made by the CNES navigation team on the probable azimuth and elevation angles of the lander antenna during the FSS.

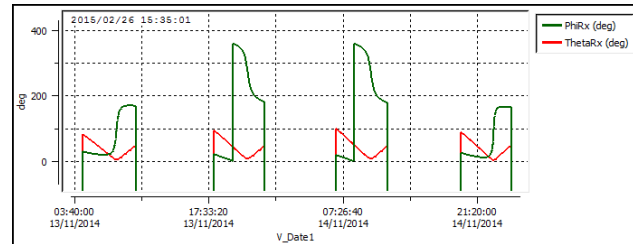


Figure 10: Lander antenna azimuth and elevation angles simulation during FSS

Interference analysis

The previous level profiles show arches visible on the **Figure 9**. As previously explained they are due to multipath interferences. During the first visibility, the arches are discernible and allow working on a model.

When a radio signal is transmitted with a direct and a reflected component, the attenuation due to the reflection interference depends on the reflection angle θ , the distance d between the antennas and the reflecting surface, the reflection coefficient of the surface and the wavelength of the signal.

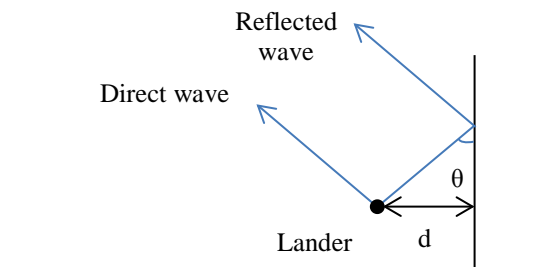


Figure 11: Wave reflection model

As the comet is in rotation and considering that the orbiter is motionless, the elevation angle θ is changing over time according to the comet period (12.4 h).

For two values of distance between antennas and the reflecting surface (40 cm and 1 m) and for a reflection coefficient taken equal to 1, the following figure gives the profile of the attenuation expectable on the direct signal.

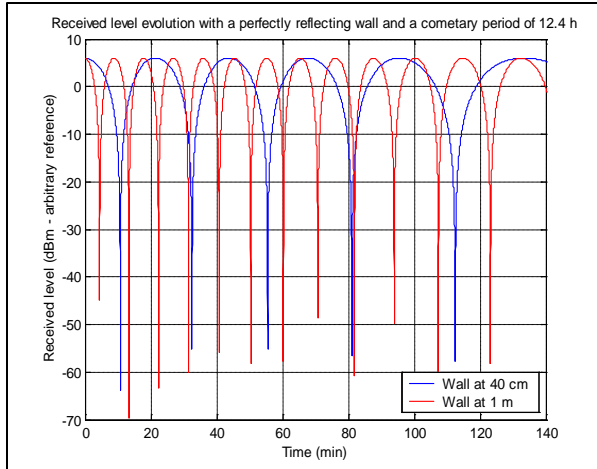


Figure 12: Variable attenuation model for reflecting surface at 1 m and 0.4 m

Customizing the distance (41.5 cm) to fit the model with the measured received power, the following figure (Figure 13) is obtained.

The simple model used for the multipath interferences does not allow making highly reliable conclusions. What can be said is that there is probably a reflecting surface situated around 40 cm of the antennas. This implies that the lander attitude is not optimal and it is oriented toward some rocks.

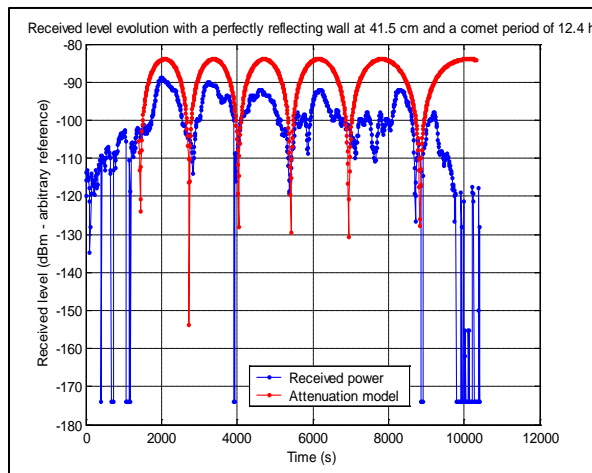


Figure 13: Comparison of attenuation model with RSSI

The model could be sharpened if the nature of the relief was known and by taking into account the orbiter speed relatively to the comet and the lander attitude.

As visible on the last three visibilities, complex interference phenomena are at stake with multiple reflected signal combined with diffraction and possibly no direct signal.

CONCLUSION

The RF link analysis of the first mission having landed a space science laboratory on a comet allowed understanding the successive events in the particular context of the rebound landing and the unknown final position. The lander spin during the rebound phase could be determined thanks to a frequency analysis of the received power on orbiter side.

When the lander has been stabilized on the ground, the RF link could be established at each orbiter-lander visibility. A propagation model derived from the power variations offers clues on the final lander attitude and position with regard to its environment.

The RF link behaved nominally when established and has played its part at best despite the difficult conditions, from the separation with the orbiter to the final hibernation on 67P/Churyumov-Gerasimenko.

GLOSSARY

- AOS: Acquisition Of signal
- CIVA: Comet Infrared and Visible Analyzer
- FSS: First Science Sequence
- RF: Radio Frequency
- ROLIS: Rosetta Lander Imaging System
- ROMAP: Rosetta Magnetometer and Plasma-monitor
- RSSI: Received Signal Strength Indicator
- SDL: Separation Descent and Landing
- TD: Touchdown